Inconsistency of basic optical processes in plasmonic nanocomposites

T. V. Shubina,[1] V. A. Kosobukin,[1] T. A. Komissarova,[1] V. N. Jmerik,[1] A. N. Semenov,[1] B. Ya. Meltser,[1] P. S. Kop'ev,[1] S. V. Ivanov,[1] A. Vasson,[2] J. Leymarie,[2] N. A. Gippius,[2,3] T. Araki,[4] T. Akagi,[4] and Y. Nanishi[4]

[1]*Ioffe Physico-Technical Institute, Russian Academy of Sciences, 194021 St. Petersburg, Russia*

[2]*LASMEA-UMR, 6602 CNRS-UBP, 63177 Cedex, France*

[3]*A. M. Prokhorov General Physics Institute, RAS, Moscow 119991, Russia*

[4]*Ritsumeikan University, 1-1-1 Noji-Higashi, Kusatsu, Shiga 525-8577, Japan*

(Received 6 February 2009; published 9 April 2009)

Plasmonic nanocomposites, comprising metallic clusters within a semiconductor matrix, exhibit a huge discrepancy between characteristic energies of luminescence, absorption, and generation of photocarriers. This phenomenon, discovered experimentally in InN/In and supported by GaAs/In data, appears because the optical processes occur in spatially different areas which undergo different influence of local plasmons. Manifestations of that in infrared emission and thermally detected absorption are considered using the formalism of electromagnetic enhancement, taking into account the statistics of cluster shapes and the transitions between parallel bands inherent for In.

DOI: 10.1103/PhysRevB.79.153105 PACS number(s): 81.07.−b, 36.40.Gk, 73.20.Mf

Rapidly developed plasmonics suggests new concepts of light manipulation and amplification.[1] Recently, it has been demonstrated that combination of metal and semiconductor can enhance the light-emission efficiency.[2] This enhancement results from the interaction of surface plasmons at metallic films or clusters (particles) with dipole transitions excited nearby.[3] The local plasmons at the clusters are effective emitters with rather high radiative decay rate[4] that amplifies recombination efficiency of coupled dipole-plasmon states.[5]

Most of previous studies dealt with the clusters situated either inside a dielectric matrix or on structure surface.[1–6] We focus on another much less investigated system—the nanocomposites, which contains metallic nanoclusters inside an optically active semiconductor host. They can be defined as an effective medium whose optical properties are governed by the plasmons. It seems to be the case of InN with spontaneously formed In clusters[7] that causes a controversy on its absorption and emission nature. Furthermore, InN has long been proposed as a promising material for full-spectrum solar cells. However, no data on the photovoltaic effect below 1.3 eV have been reported so far for unknown reason. General features of the plasmonic nanocomposites are still unclear although InN/In is suitable to study them, being a simplest binary-element system.

To provide the plasmonic effects, the well-known requirements to the metal permittivity $\varepsilon(\omega)$ at frequency ω are (i) $\mathrm{Re}\,\varepsilon(\omega)<0$ and (ii) $|\mathrm{Re}\,\varepsilon(\omega)|/\mathrm{Im}\,\varepsilon(\omega)\gg 1$. They are reasonably fulfilled for In in the infrared range [Fig. 1(a)]. Tetragonal In can easily form clusters of good crystalline structure within hexagonal InN.[8] On the other side, parallel bands emerge along certain directions due to electron-lattice interaction.[9,10] The transitions between these bands are intense near the Fermi surface [Fig. 1(b)] and might interfere with plasmons.

In this Brief Report, we state a major inconsistency in plasmonic nanocomposites related to their strong optical inhomogeneity. It manifests itself as a discrepancy between characteristic energies of basic optical processes, e.g., onsets of absorption and generation of photocarriers, which match well in a semiconductor. This inconsistency is a key to distinguish a nanocomposite from a semiconductor, in particular InN/In from InN. Without that, optimization of a structure using absorption or emission data does not guarantee, e.g., its applicability for the solar cells.

A set of InN/In structures was grown by plasma-assisted molecular-beam epitaxy at the Ioffe Institute by means of periodic deposition of pure In separated by 25 nm of InN. This permits us to be sure on the metal amount. The nominal In thickness in different samples was 0 (reference sample), 2, 4, 8, 16, and 48 monolayers (ML); one ML equals approximately 0.3 nm. Hereafter the thickness in ML is used for the sample notation. The number of the insertions was 20, except for the 48 ML sample (6 periods). All structures exhibit *n*-type conductivity with the Hall concentration around 10^{19} cm^{-3}.[11] Despite our efforts (*N*-rich growth of InN), the 0 ML_A sample of this series contains spontaneously formed clusters. Their density is estimated to be five times lower than that in the sample 0 ML_B, grown at $\mathrm{N/In}\sim 1$ and examined by transmission electron microscope (TEM) earlier.[8] Similar In planes were inserted in GaAs. The critical thick-

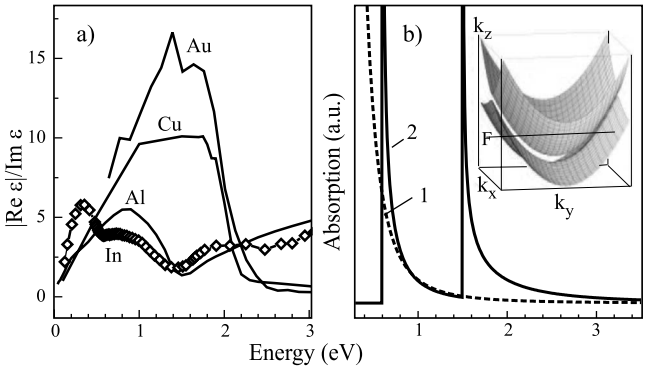

FIG. 1. (a) $|\mathrm{Re}\,\varepsilon|/\mathrm{Im}\,\varepsilon$ spectra shown for In and few other metals (Ref. 10). (b) Drude (1) and parallel-band (2) absorptions calculated for bulk In. The peaks at 0.6 and 1.5 eV correspond to (200) and (111) transitions, in notation of (Ref. 9). The insert presents the parallel bands in *k* space with the Fermi energy (*F*) shown as a guide.

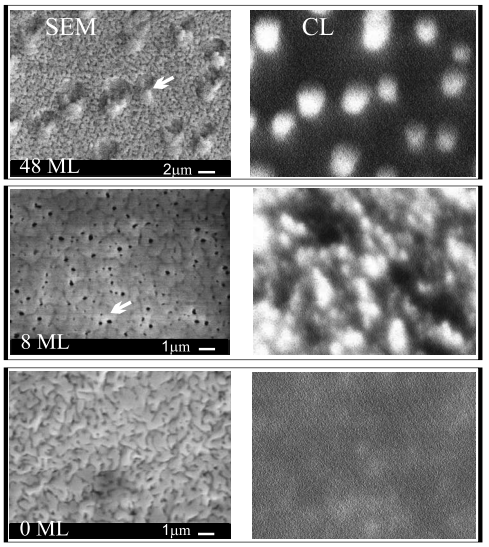

FIG. 2. SEM and CL (150 K) images taken from InN/In samples at 15 keV using a HITACHI S4300SE microscope at the Ritsumeikan University (the OXFORD CL stage with a detector sensitive from 0.6 eV and a filter cutting sapphire emission). The arrows mark In cluster agglomerations.

ness of In insertions in a semiconductor is very small (~1 ML in InN). With it exceeding, the continuous layers are transformed into clusters. Then, the small clusters are dissolved in favor of large ones, in line with Ref. 12. This promotes homogenization of the cluster shape toward more spherical and formation of cluster agglomerations, well resolved in scanning electron microscopy (SEM) images as lighter areas (Fig. 2, left).

The InN/In composites exhibit emission and absorption edges near 0.7–0.8 eV, i.e., in the range typical of InN films.[13] The striking difference is the spatial correlation of the emission sites with the In clusters, revealed by SEM and cathodoluminescence (CL) imaging of the same areas (Fig. 2). The "spot" mono-CL measurement shows difference by the factor of ~70 between the intensities at the In agglomerations and the rest area. On an average, the 48 ML sample comprising 1/3 of metal has the luminescence intensity fivefold higher than 0 ML_A.

These findings are suggestive of plasmonic effects. To reveal their influence on the basic optical processes, we have performed a comparative study of thermally detected optical absorption (TDOA) and photocurrent (PC). The TDOA is the most sensitive technique to record the nonradiative decay of plasmons accompanied by transforming their energy into heat. This effect has to be stronger below an InN absorption edge, where it is not suppressed by interband transitions. On the contrary, PC is a measure of carrier generation in the spectral range of the interband absorption in a semiconductor; it should reproduce an InN absorption onset in any case.

The PC was detected with the excitation by 100 mW semiconductor lasers of various wavelengths in a planar geometry with contacts placed on the film surface. The PC spectra were recorded at 25 K in several samples with a low In amount (Fig. 3). With an In content increase, a signal drops down by 2 orders at 1.5 eV; and it cannot be measured

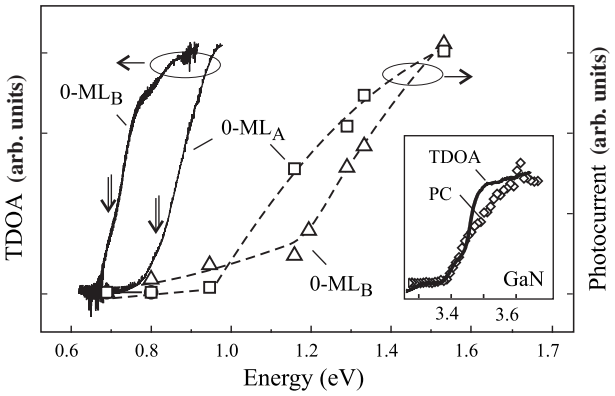

FIG. 3. PC and TDOA recorded in 0 ML_A and 0 ML_B samples having the Hall concentration 2×10^{19} cm^{-3}. The double arrows denote emission peak energies. The dashed lines are to guide the eyes. The inset shows the GaN spectra.

below. In accordance with the PC data, the absorption edge in the host is around 1–1.2 eV. The variation in the PC edge may be induced by InN nonstoichiometry, accompanying the cluster formation, due to the strong difference in the N and In atomic orbital energies.[14] The negligible PC signal below 1 eV proves that there is no density of states here because the plasmons must enhance the carrier generation in a defect band which could be due to the high impurity level. However, we cannot positively deny that the apparent PC edge might be associated with such a band.

The TDOA spectra are measured at 0.35 K in a pumped ^{3}He cryostat and normalized to those of an InAs bolometer. The TDOA edges are found to be lower in energy than PC ones (Fig. 3). Note that in GaAs/In the principal PC edge is constantly at 1.5 eV, while the TDOA is markedly extended toward lower energies. Without plasmons, the onsets of PC and TDOA coincide perfectly, as has been proved by the similar measurements of pure GaAs and GaN (Fig. 3, inset).

The TDOA and CL spectra in InN/In (Fig. 4) exhibit other features which are related to the plasmon-induced discrepancy, as will be discussed in detail in the following paragraphs. (i) The CL and TDOA peaks move to the opposite

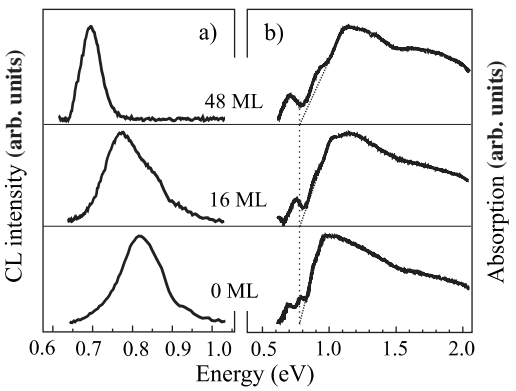

FIG. 4. (a) CL and (b) TDOA spectra recorded in different samples with the Hall concentration (in units of 10^{19} cm^{-3}): 0 ML_A - 2, 16 ML - 4.0, and 48 ML - 4.5. The dotted lines give the TDOA onsets showing a weak concentration dependence.

directions with the In increase. (ii) The emission band has frequently two components. (iii) TDOA spectra have peculiarities at the energies of parallel-band transitions, e.g., a dip at 1.5 eV.

We analyze the experimental findings in the framework of electromagnetic enhancement,[3] which implies that the local electric field E is much stronger than the external field E_0, i.e., $|g|=|E/E_0| \gg 1$. In such a field E, both emission and absorption spectra are enhanced as $|g|^2$. A metal cluster is simulated by a spheroid whose rotation axis c is parallel and two other axes, $a=b$, are perpendicular to the growth direction. Surface plasmon polarized along i-th axis of the spheroid provides at its poles the partial enhancement factor,

$$|\tilde{g}_i(\omega)| = \left| \frac{\varepsilon}{\varepsilon_1 + L_i(\varepsilon - \varepsilon_1)} \right|. \quad (1)$$

Here, $\varepsilon(\omega)$ and $\varepsilon_1(\omega)$ denote the permittivities in and out of the spheroid, L_i is the depolarizing factor dependent on the aspect ratio a/c. The factor [Eq. (1)] becomes as large as approximately $L_i^{-1}|\mathrm{Re}\ \varepsilon|/\mathrm{Im}\ \varepsilon \gg 1$ at the resonance condition $\mathrm{Re}[\varepsilon_1+L_i(\varepsilon-\varepsilon_1)]=0$ which is satisfied by the plasmon frequency $\omega_i=\omega_p/[\varepsilon_\infty+\varepsilon_1(L_i^{-1}-1)]^{1/2}$, with ω_p and ε_∞ being the plasma frequency and the background dielectric constant, respectively, of bulk metal. The local enhancement factor $|g_i(\omega,\mathbf{r})|$ as a function of position $\mathbf{r}$ outside the spheroid follows the dipolar field of i-th surface plasmon and varies from Eq. (1) at i-th poles down to about $L_i^{-1}|\mathrm{Re}\ \varepsilon_1|/\mathrm{Im}\ \varepsilon \sim 1$ at the pole of an orthogonal axis and in the spheroid interior, where the field is uniform.

The enhancement for an In cluster is estimated with the dielectric function $\varepsilon(\omega)=\epsilon_\infty+i4\pi\sigma(\omega)/\omega$, where the conductivity $\sigma=\sigma_D+\sigma_P$ includes the Drude contribution $\sigma_D(\omega)$ and the term

$$\sigma_P(\omega) = \sum_j \sigma_j \frac{\omega_j^2}{\omega\sqrt{\omega^2-\omega_j^2}}\vartheta(\omega-\omega_j), \quad (2)$$

describing absorption due to the parallel-band transitions.[9] The function σ_D is fitted using the data of Ref. 10 for In. In Eq. (2), $\omega_j=2U_j/\hbar$, where U_j is the Fourier component of the lattice pseudopotential; $\vartheta(\xi)=0$ if $\xi<0$, and $\vartheta(\xi)=1$ if $\xi>0$. We take $2U_{(200)}=0.6$ eV, $2U_{(111)}=1.5$ eV, and $\sigma_j=1\times10^{15}$ s^{-1} for both. For real crystals, to smooth the singular term in Eq. (2) we add to ω the imaginary part of 1.6×10^{14} s^{-1} equal to the damping parameter in σ_D. For demonstration, the $\varepsilon_1(\omega)$ function is chosen to match the ~1-eV optical gap of the semiconductor host.

In composites, the shape and orientation of clusters are random. To get an enhancement averaged over the ensemble, we use a model of spheroids with random ratio a/c and the same volume. Then, the inhomogeneously broadened enhancement spectrum $G(\omega)=\langle|g(\omega,\mathbf{r})|^2\rangle$ due to a total set of plasmons is obtained by spatial averaging about a spheroid followed by averaging over the spheroid shapes governed by a/c. For oblate [prolate] spheroids, their distribution function is nonzero in the interval $1 \le a/c \le (a/c)_{\max}[(a/c)_{\min} \le a/c \le 1]$, where it is presented by a part of Gaussian having the center at $a/c=1$ and a width δ [$1/\delta$]. When δ increases, the maximum in the $G(\omega)$ spectrum undergoes a low-energy shift owing to additional contributions from spheroids with smaller L_i, supporting plasmons with smaller ω_i [Fig. 5(a)]. The maximum partial enhancement $|\tilde{g}_i(\omega_i)|^2$ from Eq. (1) may be as high as 10^3-10^4 near the strongly curved surface of a single spheroid. However, because of a small relative volume of such regions and the dispersion of spheroids over a/c, the enhancement $G(\omega)$ is somewhat smaller than $\sim10^2$ at 0.7 eV, in reasonable agreement with the CL intensity contrast. Using the experimental dielectric function gives similar results.

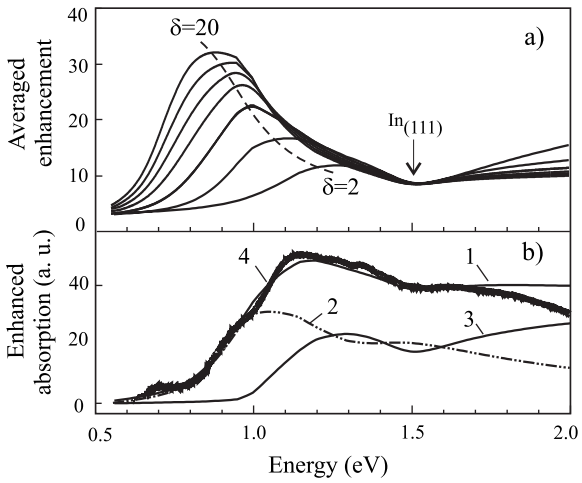

FIG. 5. (a) Averaged enhancement spectra calculated with $2<\delta<20$ and $(a/c)_{\max}=20$. (b) Enhanced absorption spectrum (1) and its constituents from clusters (2) and a host (3) calculated with $\delta=4$. Inessential interference features are subtracted in the TDOA spectrum (4).

The dissipative loss in n-th medium is $\sim\omega\ \mathrm{Im}(\varepsilon_n)|E_n|^2$. To estimate these losses (heating) in a metal cluster and a matrix, the related spectra $G(\omega)$ multiplied by $\mathrm{Im}\ \varepsilon(\omega)$ and $\mathrm{Im}\ \varepsilon_1(\omega)$, respectively, are calculated. With $\delta=4$, this sum fits reasonably the normalized TDOA in the 48 ML sample, where the area not influenced by the plasmons is negligible. One can see that the signal below the host absorption edge is exclusively associated with plasmons of the clusters [Fig. 5(b)].

The calculated spectra have a dip at 1.5 eV, which is similar to that reproducibly observed in the TDOA spectra (Fig. 4). The dip appears due to selective suppression of the plasmons by the (111) parallel-band transitions due to the imaginary part increase in $|\mathrm{Re}\ \varepsilon(\omega)|/\mathrm{Im}\ \varepsilon(\omega)$ ratio which defines the strength of plasmonic resonances. It prohibits mostly the enhancement of the semiconductor transitions in the regions adjusting to the clusters. Therefore the depth of the dip depends on a fraction of metal and its dispersion. The (200) transitions, superimposed with the strong Drude absorption, do not exhibit such a peculiarity but diminish half as much the enhancement. Both effects evidence the plasmonic enhancement implicitly; without that the absorption rise might be due to the parallel-band absorption in clusters.

Within the plasmon concept, the unusual shift of the CL and TDOA peaks in the opposite directions in Fig. 4 is not surprising since the emission and heating are dominated by different plasmonic processes. The radiative decay of plas-

mons, whose rate rises strongly on the cluster size,[4] prevails in the dense cluster agglomerations (Fig. 2), where formation of large particles is presumably facilitated. The decrease in the plasmon frequency in these regions may be due to collective interaction between local plasmons.[15] We estimated the relative frequency shift of the radiative collective plasmon mode with respect to the frequency of a single cluster to be of tens of meV. This value is well consistent with the energy difference of 50 meV between the CL lines, recorded using the "spot" regime in the adjusting regions with the agglomerated and well-separated clusters. On the contrary, the plasmon dissipation (heating) dominates in the small clusters uniformly dispersed inside the matrix. With increasing In amount, homogenization of the such cluster shapes results in δ narrowing that shifts the TDOA peak to the higher energy. The confirmation of such a scenario has been obtained by the GaAs/In studies. This system does not suffer from the instability at TEM studies, typical of InN.[8] The TEM investigation has demonstrated that with exceeding the critical thickness in GaAs/In ($\sim$5 ML) the planar arrays of the small clusters, almost round and uniform, appear along with the large cluster agglomerations. This is accompanied by the shift of the principal TDOA peak toward higher energies.

In conclusion, an essential discrepancy between characteristic energies of absorption, emission, and photocarrier generation processes is found in metal-semiconductor nanocomposites. Calculated averaged enhancement is well consistent with experimental data indicating strong plasmonic contributions to infrared emission and absorption. These results are important for optoelectronic devices of next generation based on InN and plasmonic nanocomposites.

We thank M. I. Dyakonov, M. M. Glasov, and A. Kavokin for fruitful discussions; N. A. Pikhtin, A. A. Sitnikova, and K. Kosaka for help in these studies. This work was supported by RFBR, Presidium of RAS, ANR, and the RFBR-JSPS joint program.

[1] S. A. Maier, *Plasmonics: Fundamentals and Applications* (Springer, New York, 2007).
[2] E. Ozbay, Science **311**, 189 (2006); K. Okamoto, I. Niki, A. Shvartser, Y. Narukawa, T. Mukai, and A. Scherer, Nature Mater. **3**, 601 (2004).
[3] M. Moskovits, Rev. Mod. Phys. **57**, 783 (1985).
[4] J. Crowell and R. H. Ritchie, Phys. Rev. **172**, 436 (1968).
[5] J. Gersten and A. Nitzan, J. Chem. Phys. **75**, 1139 (1981).
[6] U. Kreibig and M. Vollmer, *Optical Properties of Metal Clusters* (Springer, Berlin, 1995).
[7] T. V. Shubina, S. V. Ivanov, V. N. Jmerik, D. D. Solnyshkov, V. A. Vekshin, P. S. Kop'ev, A. Vasson, J. Leymarie, A. Kavokin, H. Amano, K. Shimono, A. Kasic, and B. Monemar, Phys. Rev. Lett. **92**, 117407 (2004); **95**, 209901 (2005).
[8] T. P. Bartel, C. Kisielowski, P. Specht, T. V. Shubina, V. N. Jmerik, and S. V. Ivanov, Appl. Phys. Lett. **91**, 101908 (2007).
[9] W. A. Harrison, Phys. Rev. **147**, 467 (1966).
[10] The data for metals are taken from In: A. I. Golovashkin, I. S. Levchenko, G. P. Motulevich, and A. A. Shubin, Zh. Eksp. Teor. Fiz. **51**, 1622 (1963); Sov. Phys. JETP **24**, 1093 (1967); Au: P. B. Johnson, and R. W. Christy, Phys. Rev. B **6**, 4370 (1972); Cu: H. J. Hagemann, W. Gudat, and C. Kunz, J. Opt. Soc. Am. **65**, 742 (1975); Al: E. Shiles, T. Sasaki, M. Inokuti, and D. Y. Smith, Phys. Rev. B **22**, 1612 (1980).
[11] T. A. Komissarova, D. S. Plotnikov, V. N. Jmerik, T. V. Shubina, A. M. Mizerov, A. N. Semenov, S. V. Ivanov, L. I. Ryabova, and D. R. Khokhlov, Phys. Status Solidi C **5**, 1621 (2008).
[12] I. M. Lifshitz and V. V. Slyozov, J. Phys. Chem. Solids **19**, 35 (1961).
[13] V. Yu. Davydov and A. A. Klochikhin, Semiconductors **38**, 861 (2004).
[14] T. V. Shubina, M. M. Glazov, S. V. Ivanov, A. Vasson, J. Leymarie, B. Monemar, T. Araki, H. Naoi, and Y. Nanishi, Phys. Status Solidi C **4**, 2474 (2007).
[15] B. N. J. Persson and A. Liebsch, Phys. Rev. B **28**, 4247 (1983).